Inorg. Chem. **1993,** *32,* 2597–2599

Synthesis, Structure, and Properties of the Novel Iron Complex of Mixed κ^3N- and κ^3O-Tripod Ligands: [*n*-Bu_4N][$(HB(pz)_3)Fe(P_3O_9)$]

Kyu-Nam Han,[†] Dongmok Whang,[†] Hae-Jeong Lee,[‡] Youngkyu Do,[‡] and Kimoon Kim*[,†]

Department of Chemistry and Center for Biofunctional Molecules, Pohang Institute of Science and Technology, P.O. Box 125, Pohang 790-600, South Korea, and Department of Chemistry and Center for Molecular Science, Korea Advanced Institute of Science and Technology, Taejon 305-701, South Korea

Received September 10, 1992

The nitrogen tripod ligand tris(1-pyrazolyl)borate ($HB(pz)_3^-$) has been widely used in the synthesis of a variety of metal complexes.[1] In contrast, very few metal complexes of the oxygen tripod ligand trimetaphosphate ($P_3O_9^{3-}$) have been reported[2] although organometallic compounds containing its congener $[CpCo\{P(O)R'R''\}_3]^-$ have been studied to some extent.[3] It would be interesting to study metal complexes containing both a nitrogen tripod ligand (L) and a oxygen tripod ligand (L′), MLL′. However, it has been difficult to synthesize such complexes partly because nitrogen tripod ligands, especially $HB(pz)_3^-$, have strong tendency to form full sandwich complexes ML_2 unless bulky substituents on the ligand prevent the formation of ML_2.[4] Recently, Fukui et al.[5a] and we[5b] independently prepared the half-sandwich complex $[Et_4N][(HB(pz)_3)FeCl_3]$, which provided us with an opportunity to synthesize iron complexes of mixed tripod ligands. Here we report synthesis, X-ray structure and properties of the novel iron (III) complex of mixed κ^3N- and κ^3O-tripod ligands, [*n*-Bu_4N][$(HB(pz)_3)Fe(P_3O_9)$] (**1**). This complex allowed us to compare the potentially useful oxygen tripod ligand $P_3O_9^{3-}$ with the well-known $HB(pz)_3^-$ ligand in terms of the coordination geometry and effects on the magnetic and electrochemical properties of the metal.

Experimental Section

All chemicals were of reagent grade and were used without further purification except as noted below. All manipulations were performed with Schlenkware and cannula techniques under an argon atmosphere. Argon was purified by passage through successive columns of activated molecular sieves 13X (Aldrich) and Ridox. $[Et_4N][(HB(pz)_3)FeCl_3]$ was prepared as described previously.[5b] CH_2Cl_2 and Et_2O were distilled from P_2O_5 and sodium benzophenone ketyl under a nitrogen atmosphere, respectively. The supporting electrolyte tetrabutylammonium perchlorate (TBAP) (Fluka) was recrystallized twice from ethanol. UV–visible and FT-IR spectra were recorded on a Hewlett-Packard 8542A spectrometer and a Bomem DA3.01 spectrometer, respectively. Room-temperature magnetic susceptibilities were measured with a Johnson Matthey magnetic susceptibility balance. The variable-temperature measurements of magnetic susceptibilities were performed on a Quantum Design MPMS SQUID magnetometer over the temperature range 6–300 K.

Table I. Crystallographic Data for [*n*-Bu_4N][$(HB(pz)_3)Fe(P_3O_9)$]

formula	$C_{25}H_{46}N_7$-BP_3O_9Fe	radiation	graphite-monochromated Mo Kα ($\lambda(K\alpha_1)$ = 0.709 26 Å)
fw	748.27	linear abs coeff, cm^{-1}	6.02
space group	$P2_12_12_1$ (No. 19)	2θ limits, deg	$4.0 \le 2\theta \le 48.0$
a, Å	11.002 (2)	no. of unique data with $I > 3\sigma(I)$	2458
b, Å	16.894 (2)	no. of variables	415
c, Å	19.433 (2)	R_F[a]	0.043
V, Å³	3612.0 (9)	R_{wF}[b]	0.051
Z	4	GOF	2.00
temp, °C	23		
d_{calc}, g/cm³	1.380		

[a] $R_F = \sum||F_o| - |F_c||/\sum|F_o|$. [b] $R_{wF} = [\sum w(|F_o| - |F_c|)^2/\sum w|F_o|^2]^{1/2}$; $w = 4F_o^2/\sigma^2(F_o^2)$; $\sigma(F_o^2) = [\sigma(I) + (pI)^2]^{1/2}$.

Synthesis of [*n*-Bu_4N][$(HB(pz)_3)Fe(P_3O_9)$] (1). A solution of (*n*-Bu_4N)(P_3O_9)[2a] (0.40 g, 0.40 mmol) in CH_2Cl_2 (10 mL) was added to a solution of $[Et_4N][(HB(pz)_3)FeCl_3]$ (0.20 g, 0.40 mmol) in CH_2Cl_2 (10 mL) under argon. After 20 min of stirring, the mixture was filtered and the volume of the filtrate was reduced to ~5 mL under reduced pressure. The product was crystallized by slowly adding Et_2O to the solution (0.49 g, 66%). UV–vis (CH_2Cl_2, nm): λ_{max} (ϵ) 344 (4200), 265 (4400). IR (KBr, cm^{-1}): 3112 (w), 2964 (m), 2876 (w), 1638 (w), 1504 (s), 1406 (m), 1330 (s), 1296 (s), 1208 (m), 1112 (s), 1054 (m), 988 (w), 944 (s), 776 (m), 713 (m), 659 (w), 621 (w), 553 (m), 442 (w). Anal. Calcd for $C_{25}H_{46}N_7BO_9P_3Fe$: C, 40.13; H, 6.20; N, 13.10. Found: C, 40.23; H, 6.17; N, 12.90.

Electrochemical Measurements. Cyclic voltammetry was performed with a EG & G 273 potentiostat and standard three electrode cells. A glassy-carbon electrode was used as the working electrode, a platinum wire as the counter electrode, and a silver wire as the pseudoreference electrode. Cyclic voltammograms were obtained on approximately 2×10^{-3} M solutions of the samples in 0.2 M TBAP in CH_2Cl_2 or CH_3CN. Ferrocene was added as an internal standard ($Cp_2Fe^{0/+}$: ~0.40 V vs Ag wire; ~0.46 V vs SCE).

X-ray Crystal Structure Determination. X-ray data were collected on an Enraf-Nonius CAD4 diffractometer using Mo Kα radiation at room temperature. Cell parameters and an orientation matrix for data collection were obtained from least-squares refinement, using the setting angles of 25 reflections in the range $20.0 < 2\theta < 30.0$. The crystallographic data are summarized in Table I. The intensities of three standard reflections, recorded every 3 h of X-ray exposure, showed no systematic changes. All the calculations were carried out with the Enraf-Nonius structure determination package MolEN. The intensity data were corrected for Lorentz and polarization effects and empirical absorption corrections (DIFABS) were also applied. The structure was solved by a combination of Patterson and difference Fourier methods and refined by full-matrix least-squares methods. All the nonhydrogen atoms were refined anisotopically. The positions of hydrogen atoms were idealized (d(C–H) = 0.95 Å) and included in the calculations of the structure factors as fixed contributions. Each hydrogen atom was assigned an isotropic thermal parameter of 1.2 times that of attached atom. The final cycle of refinement led to the *R* indices listed in Table I. The final positional and equivalent isotropic thermal parameters of the nonhydrogen atoms is given in Table II.

Results and Discussion

The novel iron (III) complex of mixed κ^3N- and κ^3O-tripod ligands, $[(HB(pz)_3)Fe(P_3O_9)]^-$ was easily synthesized by replacing the three coordinated chloride ions of $[(HB(pz)_3)FeCl_3]^-$ with a $P_3O_9^{3-}$. To our knowledge, this is the first metal complex of mixed κ^3N- and κ^3O-tripod ligands. Compound **1** has been characterized by UV–vis and IR spectroscopy and elemental analysis. Coordination of a $P_3O_9^{3-}$ ligand to the metal ion in a κ^3O fashion was indicated by the splitting of the strong band near 1300 cm^{-1} due to $P_3O_9^{3-}$ into two bands in the IR spectrum, a

---

[†] Pohang Institute of Science and Technology.

[‡] Korea Advanced Institute of Science and Technology.

(1) (a) Trofimenko, S. *Prog. Inorg. Chem.* **1986**, *34*, 115. (b) Shaver, A. In *Comprehensive Coordination Chemistry*; Wilkinson, G., Gillard, R. D., MacCleverty, J. A., Eds.; Pergamon: Oxford, England, 1987; Vol. 2, p 245.

(2) (a) Besecker, C. J.; Day, V. W.; Klemperer, W. G. *Organometallics* **1985**, *4*, 564. (b) Day, V. W.; Klemperer, W. G.; Main, D. J. *Inorg. Chem.* **1990**, *29*, 2345. (c) Day, V. W.; Klemperer, W. G.; Lockledge, S. P.; Main, D. J. *J. Am. Chem. Soc.* **1990**, *112*, 2031. (d) Ryu, S.; Whang, D.; Kim, J.; Yeo, W.; Kim, K. *J. Chem. Soc., Dalton Trans.* **1993**, 205.

(3) For a review: Klaui, W. *Angew. Chem., Int. Ed. Engl.* **1990**, *29*, 627.

(4) (a) Calabrese, J. C.; Domaille, P. J.; Thompson, J. S.; Trofimenko, S. *Inorg. Chem.* **1990**, *29*, 4429. (b) Trofimenko, S.; Calabrese, J. C.; Domaille, P. J.; Thompson, J. S. *Ibid.* **1989**, *28*, 1091. (c) Trofimenko, S.; Calabrese, J. C.; Thompson, J. S. *Ibid.* **1987**, *26*, 1507.

(5) (a) Fukui, H.; Ito, M.; Moro-oka Y.; Kitajima, N. *Inorg. Chem.* **1990**, *29*, 2868. (b) Cho, S.-H.; Whang, D.; Han, K.-N.; Kim, K. *Ibid.* **1992**, *31*, 519.

0020-1669/93/1332-2597$04.00/0

Table II. Positional and Equivalent Isotropic Thermal Parameters of Non-Hydrogen Atoms for $[n\text{-}Bu_4N][(HB(pz)_3)Fe(P_3O_9)]$

atom	x	y	z	B_{eq}, Å^2
Fe	0.57252(8)	0.06831(6)	0.95209(5)	2.80(1)
P1	0.4289(2)	−0.0523(1)	1.0426(1)	3.52(3)
P2	0.6847(2)	−0.0498(1)	1.0587(1)	3.34(3)
P3	0.5414(2)	0.0744(1)	1.11249(9)	3.28(3)
O1	0.4413(4)	−0.0087(3)	0.9752(3)	3.39(9)
O2	0.6958(4)	−0.0062(3)	0.9908(2)	3.27(9)
O3	0.5535(4)	0.1181(3)	1.0451(3)	3.28(9)
O4	0.5577(4)	−0.0965(3)	1.0562(3)	3.55(9)
O5	0.6566(4)	0.0152(3)	1.1177(3)	3.4(1)
O6	0.4316(4)	0.0128(3)	1.1034(3)	3.7(1)
O7	0.3297(5)	−0.1080(4)	1.0515(4)	5.4(1)
O8	0.7812(5)	−0.1029(4)	1.0806(3)	5.2(1)
O9	0.5286(6)	0.1193(4)	1.1759(3)	5.0(1)
N1	0.6917(5)	0.1615(4)	0.9309(3)	3.7(1)
N2	0.4443(5)	0.1368(4)	0.8994(3)	3.9(1)
N3	0.6212(5)	0.0272(5)	0.8539(3)	3.7(1)
N4	0.6957(6)	0.1954(5)	0.8674(4)	4.4(1)
N5	0.4749(6)	0.1770(5)	0.8422(4)	4.8(2)
N6	0.6274(6)	0.0779(5)	0.8010(3)	4.3(1)
N7	0.4226(6)	0.1372(4)	0.4033(4)	3.8(1)
C1	0.7799(7)	0.1939(5)	0.9679(5)	4.3(2)
C2	0.8412(8)	0.2494(6)	0.9284(6)	5.6(2)
C3	0.7849(9)	0.2481(6)	0.8661(6)	5.8(2)
C4	0.3283(7)	0.1563(7)	0.9137(5)	4.9(2)
C5	0.2866(8)	0.2111(8)	0.8649(6)	6.2(2)
C6	0.3811(9)	0.2227(7)	0.8211(5)	6.2(2)
C7	0.6613(8)	−0.0420(6)	0.8311(5)	4.7(2)
C8	0.6961(9)	−0.0368(7)	0.7638(5)	5.5(2)
C9	0.6711(8)	0.0403(7)	0.7456(5)	5.1(2)
C10	0.4865(7)	0.0608(6)	0.4263(5)	4.5(2)
C11	0.4247(9)	0.0124(6)	0.4808(6)	5.9(2)
C12	0.4872(9)	−0.0597(8)	0.4943(8)	7.4(3)
C13	0.441(1)	−0.1108(8)	0.5512(8)	8.5(3)
C14	0.3012(7)	0.1161(6)	0.3677(5)	4.4(2)
C15	0.3034(8)	0.0591(7)	0.3099(5)	5.6(2)
C16	0.1777(9)	0.0497(9)	0.2789(7)	7.0(3)
C17	0.172(1)	−0.012(1)	0.2237(8)	8.5(4)
C18	0.5057(7)	0.1790(5)	0.3525(5)	4.1(2)
C19	0.4571(8)	0.2522(5)	0.3209(5)	4.4(2)
C20	0.5503(9)	0.2934(6)	0.2773(6)	5.6(2)
C21	0.505(1)	0.3676(8)	0.2428(8)	7.3(3)
C22	0.3946(7)	0.1897(6)	0.4640(5)	4.6(2)
C23	0.5004(9)	0.2182(6)	0.5056(6)	5.4(2)
C24	0.461(1)	0.2642(9)	0.5692(5)	8.5(4)
C25	0.420(2)	0.219(1)	0.6237(9)	13.7(6)
B	0.606(1)	0.1668(7)	0.8123(5)	4.9(2)

[a] Values for anisotropically refined atoms are given in the form of the equivalent isotropic thermal parameters defined as $B_{eq} = (4/3)\sum_i\sum_j\beta_{ij}\mathbf{a}_i\cdot\mathbf{a}_j$.

common feature of all the known metal complexes containing the κ^3O-P_3O_9 ligand.[2a] The structure has been confirmed by X-ray analysis.

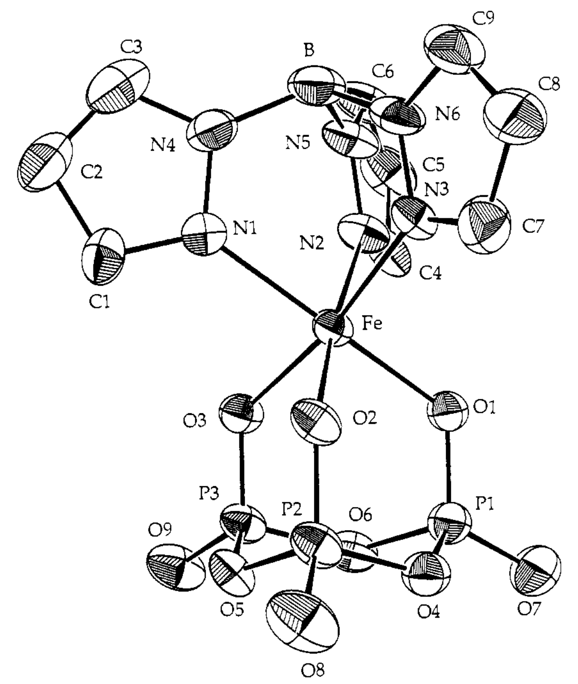

Figure 1. Structure of $[(HB(pz)_3)Fe(P_3O_9)]^-$ in **1**.

Table III. Selected Bond Distances(Å) and Angles (deg) for $[n\text{-}Bu_4N][(HB(pz)_3)Fe(P_3O_9)]$

Fe–O1	1.993(5)	Fe–N1	2.088(7)
Fe–O2	1.996(5)	Fe–N2	2.091(6)
Fe–O3	2.002(5)	Fe–N3	2.097(6)
O1–Fe–O2	89.7(2)	O2–Fe–N3	87.7(2)
O1–Fe–O3	89.8(2)	O3–Fe–N1	85.8(2)
O2–Fe–O3	89.8(2)	O3–Fe–N2	97.9(2)
O1–Fe–N1	171.8(2)	O3–Fe–N3	170.0(2)
O1–Fe–N2	89.0(2)	N1–Fe–N2	84.8(3)
O1–Fe–N3	99.9(2)	N1–Fe–N3	84.9(3)
O2–Fe–N1	97.1(2)	N2–Fe–N3	84.9(3)
O2–Fe–N2	172.2(2)		

The coordination geometry around Fe in $[Fe(P_3O_9)(HB(pz)_3)]^-$ (Figure 1) may be best described as a distorted octahedron with a face occupied by three O atoms of $P_3O_9^{3-}$ and the opposite face occupied by three N atoms of the $HB(pz)_3^-$ ligand; the approximate point group symmetry of the anion is C_{3v}. Selected bond distances and angles are listed in Table III. The $P_3O_9^{3-}$ ligand binds to the metal at shorter distances with larger bite angles than the $HB(pz)_3^-$ does: the average values for the three equivalent Fe–O distances and O–Fe–O angles are 1.997(5) Å and 89.8(2)° while the average Fe–N distance and N–Fe–N angle are 2.092(7) Å and 84.9(3)°. The equilateral triangles defined by the three coordinating N atoms and O atoms, respectively, have essentially the same lateral distances (2.823(10) and 2.818(7) Å, respectively). The two triangles are almost parallel (dihedral angle 2(4)°) and twisted by ~50°; the Fe atom is located closer to the O triangle (1.311 Å away from the N triangle and 1.158 Å from the O triangle) to form the shorter Fe–O bonds. The average Fe–N distance is much longer than that in low-spin $[Fe(HB(pz)_3)_2](NO_3)$[6] (1.954(5) Å) and somewhat shorter than that in high-spin $[Et_4N][(HB(pz)_3)FeCl_3]$[5] (2.160(11) Å). Other bond parameters for the $HB(pz)_3^-$ and $P_3O_9^{3-}$ ligands are not exceptional. The P–O bonds for the O atoms that bridge P and Fe atoms ($(P\text{–}O_c)_{av}$ = 1.510(5) Å) are somewhat longer than the terminal P–O bonds ($(P\text{–}O_t)_{av}$ = 1.452(6) Å) but are much shorter than those for the O atoms that bridge two P atoms ($(P\text{–}O_b)_{av}$ = 1.612(7) Å).

The high-spin nature of complex **1** has been confirmed by the magnetic susceptibility measurement in the solid state at room temperature (μ_{eff} = 5.6 μ_B) which is consistent with the rather long Fe–N bond distance. Although at the beginning, we suspected **1** may exhibit spin-crossover behavior, the temperature dependence of the magnetic susceptibility of **1** in the range 6–300 K closely follows the Curie law. It is interesting to note that $[Fe(HB(pz)_3)_2](NO_3)$[6] is low spin (μ_{eff} = 2.15 μ_B) while $[Et_4N]_3[Fe(P_3O_9)_2]$[7] is high spin (μ_{eff} = 5.7 μ_B). Apparently, replacing a $HB(pz)_3$ of $[Fe(HB(pz)_3)_2]^+$ with a weaker field ligand $(P_3O_9)^{3-}$ causes the change of the spin state from low spin to high spin.

Electrochemical properties of **1** were studied by cyclic voltammetry. The complex undergoes a reversible one-electron reduction at −0.57 V vs $Cp_2Fe^{0/+}$ in CH_2Cl_2, which was assigned to the reduction from Fe^{3+} to Fe^{2+}. In comparison, the $Fe^{3+/2+}$

---

(6) Cho, S.-H.; Whang, D.; Kim, K. *Bull. Kor. Chem. Soc.* **1991**, *12*, 107.

(7) We have synthesized the sandwich type metal complexes of $P_3O_9^{3-}$, $[M(P_3O_9)_2](NEt_4)_n$ (n = 4 for M = Mn^{2+}, Co^{2+}, Ni^{2+}, Cu^{2+}, Zn^{2+}; n = 3 for M = Fe^{3+}): Lee, H.-J.; Whang, D.; Kim K.; Do, Y. Manuscript in preparation.

couples of $[Fe(HB(pz)_3)_2](NO_3)$ (in CH_2Cl_2) and $[Et_4N]_3[Fe(P_3O_9)_2]$ (in CH_3CN) were measured to be −0.245 and −0.97 V vs $Cp_2Fe^{0/+}$, respectively, under the same or similar conditions. Such a large shift of the $Fe^{3+/2+}$ couple to more negative potential upon replacement of $HB(pz)_3$ with $(P_3O_9)^{3-}$ demonstrates that the more negatively charged ligand $(P_3O_9)^{3-}$ is much more effective in stabilizing the higher oxidation state.

In summary, we have synthesized and characterized the novel iron (III) complex of mixed κ^3N- and κ^3O-tripod ligands, $[n\text{-}Bu_4N][(HB(pz)_3)Fe(P_3O_9)]$ (1). This work demonstrates that compared to $HB(pz)_3^-$, the $P_3O_9^{3-}$ ligand (i) binds to Fe^{3+} at shorter distances with larger bite angles, (ii) is a weaker field ligand, and (iii) is more effective in stabilizing a higher oxidation state. Metal complexes of unusually high oxidation states may be therefore synthesized with the $P_3O_9^{3-}$ ligand(s). Work along this line is in progress in our laboratories.

Acknowledgment. We gratefully acknowledge the support from the Korea Science and Engineering Foundation. We are grateful to Dr. N. H. Hur for providing us with the preparation procedure of $(n\text{-}Bu_4N)(P_3O_9)$. We also thank the Pohang Institute of Science and Technology (POSTECH) for the partial support of the X-ray analysis.

Supplementary Material Available: A detailed X-ray crystallographic data table and complete listings of bond distances and angles and anisotropic thermal parameters (7 pages). Ordering information is given on any current masthead page.